Pharmaceutical Biology

ISSN: 1388-0209 (Print) 1744-5116 (Online) Journal homepage: informahealthcare.com/journals/iphb20

Formulation, characterization, and geno/cytotoxicity studies of galbanic acid-loaded solid lipid nanoparticles

Morteza Eskandani, Jaleh Barar, Jafar Ezzati Nazhad Dolatabadi, Hamed Hamishehkar & Hossein Nazemiyeh

To cite this article: Morteza Eskandani, Jaleh Barar, Jafar Ezzati Nazhad Dolatabadi, Hamed Hamishehkar & Hossein Nazemiyeh (2015) Formulation, characterization, and geno/cytotoxicity studies of galbanic acid-loaded solid lipid nanoparticles, Pharmaceutical Biology, 53:10, 1525-1538, DOI: 10.3109/13880209.2014.991836

To link to this article: https://doi.org/10.3109/13880209.2014.991836

Published online: 08 Apr 2015.

Pharmaceutical Biology

http://informahealthcare.com/phb
ISSN 1388-0209 print/ISSN 1744-5116 online
Editor-in-Chief: John M. Pezzuto
Pharm Biol, 2015; 53(10): 1525–1538
 DOI: 10.3109/13880209.2014.991836

informa
healthcare

ORIGINAL ARTICLE

Formulation, characterization, and geno/cytotoxicity studies of galbanic acid-loaded solid lipid nanoparticles

Morteza Eskandani[1,2], Jaleh Barar[1,3], Jafar Ezzati Nazhad Dolatabadi[1,2], Hamed Hamishehkar[4], and Hossein Nazemiyeh[1,3]

[1]*Research Center for Pharmaceutical Nanotechnology, Tabriz University of Medical Sciences, Tabriz, Iran,* [2]*Student Research Committee, Tabriz University of Medical Sciences, Tabriz, Iran,* [3]*Faculty of Pharmacy, Tabriz University of Medical Sciences, Tabriz, Iran, and* [4]*Drugs Applied Research Center, Tabriz University of Medical Sciences, Tabriz, Iran*

Abstract

Context: Galbanic acid (GBA) is a sesquiterpene coumarin with different medicinal properties and anticancer effects.

Objective: To improve the anticancer activities of GBA, in the current study, we aimed to fabricate GBA-loaded solid lipid nanoparticles (GBA-SLNs) and study their biological activities *in vitro*.

Materials and methods: Hot homogenization was used for preparation of GBA-SLNs. The encapsulation efficiency (EE) and drug loading (DL) and *in vitro* release were determined. MTT, DAPI, DNA fragmentation, comet, and Anexin V apoptosis assays were used to compare the anti-cell proliferation and genotoxicity properties of GBA and GBA-SLNs against A549 cells and HUVEC to detect apoptosis and DNA damage in the final concentration of 100 μM after 48 h treatment.

Results: Scanning electron microscopy (SEM) and particle size analysis showed spherical SLNs (92 nm), monodispersed distribution, and zeta potential of −23.39 mV. High EE (>98%) and long-term *in vitro* release were achieved. The stability of GBA-SLNs in aqueous medium was approved after 3 months in terms of size and polydispersity index. GBA was able to inhibit A549 growth with an IC_{50} value of 62 μM at 48 h. Although GBA-SLNs could also inhibit the growth rate of A549 cells, the effect is perceived after 48 h, as approved by the quantitative expression of *Bcl-xL* and *Casp 9* genes, and also genotoxicity assays.

Conclusion: Long-term apoptotic effect of GBA-SLNs compared with GBA may be due to the accumulation of GBA-SLNs in the tumor site because of deviant tumor pathology. Our data confirmed that SLNs could be exploited for sustained lipophilic GBA delivery.

Keywords

Anticancer, *Ferula ovina*, galbanic acid, sesquiterpene coumarin, sustained drug delivery

History

Received 9 June 2014
Revised 10 October 2014
Accepted 21 November 2014
Published online 8 April 2015

Introduction

Formulation of the lipophilic and sparingly soluble natural compounds using appropriate carriers is an effective strategy to overcome solubility problem and to improve their pharmacological efficiency (Schwarz & Mehnert, 1999). Solid lipid nanoparticles (SLNs) are colloidal drug carrier systems with particles of nanometer size, which consist of solid lipid matrix. SLNs possess high biocompatibility and biodegradability which are considered as suitable carriers for both hydrophilic and lipophilic compounds with a possibility of tumor passive targeting (Kheradmandnia et al., 2010). SLNs production includes a simple homogenization and solidification procedure that would enable successful scale up for industry (Rostami et al., 2014). Moreover, compared with other nano-emulsions, which are prepared with liquid lipid, SLNs show more controlled drug release potency (Das et al., 2012). The advantages of SLNs are (a) protection of incorporated compound against chemical degradation, (b) biocompatibility of the carrier, and (c) avoidance of organic solvent during formulation (Tiyaboonchai et al., 2007). The drug could be released from SLNs by different mechanisms including diffusion, polymer matrix swelling, and the polymer erosion or degradation (Zur Mühlen et al., 1998). The lipophilic nature of the SLNs, their high resemblance to the lipid bilayer of the cell membrane as well as their biocompatibility provides a great potential for delivery of lipophilic herbal remedies (Mehnert & Mäder, 2001). Delivery of lipophilic natural compounds by SLNs is a promising strategy that has attracted the attention of both phytochemist and pharmaceutical scientist to overcome their poor solubility, and to increase their pharmaceutical behaviors. In this context, fabrication of various active natural compounds such as acetylshikonin (Eskandani & Nazemiyeh, 2014),

Correspondence: Hossein Nazemiyeh, Professor of Pharmacognosy, Research Center for Pharmaceutical Nanotechnology, Tabriz University of Medical Sciences, Tabriz, Iran. Tel: +98 41 3336 7014. Fax: +98 41 3336 7929. E-mail: Nazemiyehh@tbzmed.ac.ir

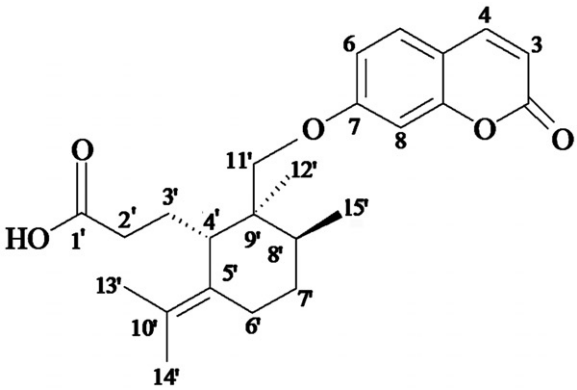

Figure 1. Chemical structure of galbanic acid.

curcumin (Wang et al., 2012), frankincense and myrrh essential oils (Shi et al., 2012), tetrandrine (Li et al., 2006), and andrographolide (Parveen et al., 2013) in SLNs have been reported until now. Apparently, however, no investigation has been made to deliver galbanic acid (GBA) to the cancerous cells by the SLNs until now.

GBA ($C_{24}H_{30}O_5$: 2-cyclohexene-1-butanoic acid) (Figure 1) is a lipophilic sesquiterpene coumarin (Bedniak, 1962) with many different medicinal properties, previously isolated from the roots of different *Ferula* species (Apiaceae) that are distributed throughout the Mediterranean and Central Asia (Iranshahi et al., 2007; Zhang et al., 2012). To date, there has been little agreement on the anticancer effects of GBA. Although the exact mechanism remains unclear, GBA may exert its anticancer activity in association with antiangiogenic action through inhibition of vascular endothelial growth factor, VEGF, and antiproliferative actions through the decrease of phosphorylation of p38-mitogen-activated protein kinase (MAPK) (Kim et al., 2011). In addition, GBA compared with verapamil, the well-known inhibitor of permeability glycoprotein (P-gp) or multidrug resistance protein 1 (MDR1), significantly inhibited the P-gp activity (Hanafi-Bojd et al., 2011). Therefore, GBA can increase the permeability of the cancerous cells to chemical medicine during chemotherapies through inhibition of multidrug resistance protein 1.

Interesting anticancer effects of GBA and poor solubility during biological evaluation due to its lipophilic properties led us to optimize for the first time a novel GBA-loaded solid lipid nanoparticles (GBA-SLNs) composed of precirol® ATO 5 as a lipid matrix to improve the pharmacokinetic behavior. GBA-SLNs were physicochemically and morphologically characterized by means of zetaseizer and scanning electron microscopy (SEM). Geno- and cytotoxicity impacts were evaluated using *in vitro* cell culture models on human epithelial A549 cells and endothelial HUVEC to compare anticancer properties of the formulations and plain GBA.

Materials and methods

Chemicals and reagents

A549 and HUVEC (human umbilical vein endothelial cells) cell lines were provided by National cell bank of Iran, Pasteur Institute (Tehran, Iran). All cell culture plates and flasks were obtained from IWAKI (CITY, Japan). RPMI1640 medium, low, and normal melting point agarose and fetal bovine serum (FBS) were bought from Gibco, Invitrogen (Paisley, UK) and Trypsin-EDTA (0.02–0.05%), Tri-Reagent, Dithiotheritol (DTT) was acquired from Sigma Aldrich Co. (Poole, UK). Precirol® ATO5 was obtained from Gattefosse (Nanterre, France). Annexin V-FITC apoptosis detection kit, RNeasy mini Kit, and Power SYBR Green PCR Master Mix were purchased from Oncogene Research Products (San Diego, CA), Qiagen (Qiagen, Hilden, Germany), and Applied Biosystems (Foster City, CA). Other chemicals, not mentioned above, were of highest quality provided by either Sigma-Aldrich (Poole, UK) or Merck Co (Darmstadt, Germany).

GBA extraction

As a part of our local medicinal plants screening program for their potential anticancer activity, we attempted to evaluate *Ferula ovina* chemical composition and bioactivities. GBA was isolated based on a bioassay-guided platform and recognized as the most anticancer component of dichloromethane extract of the *F. ovina* roots. The purity of the GBA was characterized using high-performance liquid chromatography and 1D and 2D nuclear magnetic resonance techniques.

Preparation of GBA-SLNs

GBA-SLNs were prepared by the hot homogenization method (Mehnert & Mäder, 2001; Müller et al., 2000). In brief, GBA was added to the glyceryl palmitostearate (Precirol® ATO 5) and the mixture was simply dispersed by indirect heating at approximately 10 °C above the melting point of the lipid (66 °C). An aqueous phase was prepared by dissolving the stabilizers (Poloxamer 407) in distilled water and heating to the same temperature of the oil phase. The hot aqueous phase was then added dropwise (during 45 min) to the oil phase and homogenization was performed (at 12 000 rpm and 66 °C) using a homogenizer (Heidolph Silent Crusher M GmbH & Co, Schwabach, Germany). The resultant emulsion was further homogenized (at 19 000 rpm) for additional 15 min. GBA-SLNs were finally obtained by allowing the hot nanoemulsion to cool down at room temperature, and then were stored at 4 °C. Blank SLNs also were prepared by the same method except instead of GBA, an equal amount of precirol was used.

Size, zeta potential, and morphological characteristics of nanoparticles

Size distribution was determined by laser diffraction (SALD-2100, Shimadzu Corporation, Kyoto, Japan) and a Malvern Zetasizer (3000HS, Malvern Instruments, Worcestershire, UK) recorded zeta potentials after 20 times dilution with the original dispersion medium. For morphological analysis, the samples were applied to a thin 1 cm^2 glass slide and allowed to air dry, and coated with a thin layer of gold using a direct current sputter (EMITECH K450X, England, UK). The particles were evaluated by a scanning electron microscope (MV2300, Brno, Czech Republic).

Encapsulation efficiency, drug loading, and drug content (%)

Encapsulation efficiency (EE%) was calculated by quantifying the concentration of un-entrapped GBA in aqueous medium (Luo et al., 2006). The aqueous medium was separated by ultra-filtration of SLNs using Amicon Ultra-15 Centrifugal Filter Units (EMD Millipore Corporation, Billerica, MA), which consists of filter membrane (molecular weight cutoff 10 kDa). One milliliter of the formulation containing 0.3% Tween 80 (to dissolve the un-entrapped GBA in aqueous phase) was centrifuged at 5000 rpm for 10 min. The SLNs along with encapsulated drug remained in the outer chamber and the aqueous phase moved into the sample recovery chamber through a filter membrane. Afterwards, the equal volume of chloroform was added to the aqueous phase to dissolve the intact GBA. In the final step, the aqueous phase was removed and the excess solvent was dried. Then the residual was dissolved in acetone and quantified by HPLC. The HPLC system was utilized for drug separation and elution time program was as follows: 0–20 min, methanol/acetonitril (10% v/v) from 80 to 95% in H_2O; 20–30 min, 95% methanol/acetonitril (10% v/v) in H_2O; 36 min, methanol/acetonitrile (10% v/v) 80% in H_2O. The flow rate and the UV wavelength were 1.0 ml min^{-1} and 325 nm, respectively. A calibration curve for pure GBA was plotted using different concentrations of compounds (100–4000 μg/ml; linear correlations: $R^2 = 0.994$ in acetone) and the GBA content was determined using the obtained standard curve. The EE, drug loading (DL), and drug content (%) were calculated (Luo et al., 2006) by the following equations:

$$\%\ Entrapment\ efficiency = \frac{(total\ amount\ of\ drug\ taken) - (un\text{-}entraped\ drug)}{concentration\ of\ drug\ initially\ taken} \times 100 \quad (1)$$

$$Drug\ loading\ (mg/g) = \frac{W_{GL}}{W_{NP}} \quad (2)$$

$$Drug\ concent\ (\%) = \frac{total\ GBA - free\ GBA}{W_{NP}} \quad (3)$$

where W_{GL} is the weight of GBA loaded in nanoparticles and W_{NP} is the weight of nanoparticles solid mass.

In vitro release, drug leakage, and release kinetics analysis

To study drug leakage, formulations were stored at 4 °C and 24 ± 2 °C (Suresh et al., 2007) and the drug content was estimated after 3 months, to find any change in the EE. The percentage of the leaked GBA was calculated based on the initial weight of the drug incorporated in the SLNs.

The *in vitro* release of GBA from formulated SLNs dispersions was determined using the dialysis bag diffusion technique (Huang et al., 2008). Briefly, 1 ml of GBA-SLNs with the precise concentration of GBA was transferred to a dialysis bag (a pore size of 2.4 nm). Due to the solubility limitation of GBA in aqueous solutions, the releasing aqueous medium was prepared by adding 0.3% Tween 80 (Han et al., 2009). Briefly, the bag was sealed and suspended in a beaker containing 10 ml of medium and stirred at a constant speed of 50 rpm at 37 ± 0.5 °C and 24 ± 2 °C (pHs: 5.6 and 7.4). At pre-determined time intervals, 1 ml of dissolution medium was taken and an equal amount of fresh medium was added back to the beaker and the GBA content of each sample was estimated using HPLC. The control nanoparticle formulation without GBA was treated similarly and used as a blank for the measurements. Plain GBA was also dialyzed in the same condition to assess the permeability of the drug to the membrane. The experiments were carried out in triplicate and the release data were analyzed using various kinetics models, as described previously (Matthaiou et al., 2014).

Physical stability studies

The prepared SLNs was divided to two samples and stored for 3 months in a glass tube in refrigerator (4 °C) and room temperature (24 °C). Then some physiochemical properties of SLNs including mean diameter, polydispersity index, and EE were measured and compared with the fresh ones (Ghaffari et al., 2011). All reported data are the mean of three separate measurements.

Cell culture

The cell lines were cultured into flasks and kept in a humidified incubator with 5% CO_2 at 37 °C. Human A549 cell line was grown in the 1640 medium supplemented with 10% (v/v) fetal bovine serum and antibiotics (100 mg/ml penicillin–streptomycin). Human HUVEC as normal cell lines were cultured in the RPMI 1640 medium containing glutamine, 20% FBS. Various concentrations of GBA were prepared in cultural medium containing DMSO as a co-solvent (not more than 0.3%). Plain GBA and GBA-SLNs were sterilized by filtration methods using a 0.22-μm syringe filter (JET BIOFIL, Interlab Ltd, Dunedin, New Zealand) prior to each experiment.

Cell viability assay

MTT assay was utilized to determine the cytotoxic effect of GBA and GBA-SLNs. Cells were seeded in 96 well plates and allowed to attach overnight and then were treated with various concentrations of free and GBA-loaded SLN. Nanoparticle-treated cells were considered as a control and 5% DMSO was added to the media as a positive control. After incubation period (24, 48, and 72 h), 50 μl of the MTT reagent (2 mg/ml in PBS) was added to each well and incubated in 37 °C for an additional 4 h in a humidified CO_2 incubator. After 4 h incubation, the formazan crystals were dissolved in DMSO and the UV absorbance was measured at 570 nm using a spectrophotometric plate reader, ELx 800 (Biotek, San Francisco, CA) (Eskandani et al., 2013).

Genotoxicity assays procedure

All genotoxicity assays including Anexin V apoptosis assay, DNA fragmentation, comet, and DAPI staining assays were carried out following 48 h exposure to 200 μM H_2O_2 (as a positive control), 40 μg/ml (100 μM) of GBA, and a same final concentration of GBA loaded on SLNs (v/v %).

DAPI staining

DNA condensation and fragmentation as two major characteristics of apoptosis were evaluated by DAPI staining. Briefly, A549 cells and HUVEC were seeded in six-well plates (5×10^4 cells/well), and consequently treated with GBA, GBA-SLNs, and with H_2O_2 as a positive control for 48 h. Then, the cells were washed with PBS and fixed with 4% paraformaldehyde for 1 h at RT. The cells were washed three times with PBS, permeabilized with 0.1% (w/v) Triton X-100 for 5 min, washed once more with PBS and stained by incubation with 200 ng/ml DAPI for 20 min (Hamishehkar et al., 2014) and analyzed under fluorescence microscopy (Olympus IX81, Olympus, Hamburg, Germany).

DNA fragmentation assay

The impact of GBA and its SLNs on DNA fragmentation/cleavage, as one of the important mechanistical properties of apoptotic cells, was studied. A549 cells and HUVEC were exposed to treatments for 48 h and then were incubated in the lysis buffer [50 mM Tris-base buffer, 10 mM EDTA, 0.5% sodium dodecyl sulfate (SDS), and 5 units RNase at 37 °C (pH 7.4)]. Proteins were then denaturized with 500 µl of chloroform/isoamyl alcohol (24:1) and total DNA was separated by centrifugation at 12 000 rpm. Entire DNAs were precipitated with isopropranol and was electrophoresed in 1.2% agarose gel (Nath et al., 2013).

Alkaline comet assay

To evaluate the direct interaction of drugs with the whole chromatin and DNA breakage, comet assay was performed. Cells were cultured after 48 h post-treatment; they were subjected to comet assay based on our previous works (Eskandani et al., 2010; Singh et al., 1988). Briefly, normal melting point agarose (1.5%) coated slides were used as a surface for the cells embedded in low melting point agarose (0.5%). Then cells were lysed [4 h incubation at 4 °C in the lysis buffer composed of 2.5 M NaCl, 100 mM Na_2EDTA, and 1% triton X-100 (pH 10.5)], without third agarose layer (Vandghanooni & Eskandani, 2011). Afterwards, they were placed in an ice-cold electrophoresis chamber containing 300 mM NaOH and 1 mM Na_2EDTA (pH>13) for 30 min to allow DNA unwinding and histones to be removed. This was followed by 20 min electrophoresis at 300 mA and 30 V. Next, the slides were washed with neutralization buffer (40 mM Tris-HCl, pH 7.5) and stained with a drop of ethidium bromide. Prior to slides coverage with a cover slip, they were washed two or three times to remove excess staining solution. Finally, immediate microscopic analyses (Olympus IX81 fluorescence microscope (Olympus, Hamburg, Germany) equipped with XM10 monochrome camera; wavelength 546 nm; barrier 580 nm) were performed (Eskandani et al., 2010; Singh et al., 1988) and images were analyzed by CASP software (HealthStats, Singapore, Singapore). DNA strand breaks were expressed as the percentage of total fluorescence DNA migrated in the tail for each nucleus

$$DNA\ strand\ cleavage\ \% = \frac{DNA\ in\ tail}{DNA\ in\ head} \times 100 \quad (4)$$

Annexin V apoptosis assay

The extent of apoptotitic cells after exposure to GBA (intact/SLNs) was determined by annexin V staining. Annexin V is a phospholipid-binding protein with high affinity for phosphatidylserine, which translocate from the inner sheet to the external cell surface concurrent with early apoptosis event (Van Engeland et al., 1998). In this study, annexin V-fluorescein isothiocyanate (FITC) apoptosis detection kit was used according to the protocol of the manufacturer. Briefly, treated cells were washed gently three times with PBS, detached by tripsinization, and washed three times with 500 µl 1 × binding. The supernatant was then removed and the cells were resuspended in 100 µl of annexin V-binding buffer and 8 µl of annexin V-FITC. Following 15 min incubation at room temperature in the dark, the cells were centrifuged (1000 RPM, 5 min). After removal of the supernatant, 100 µl of annexin V-binding buffer and 8 µl propidium iodide (PI) staining solution were added and incubated for 5 min at room temperature in the dark and then cells were washed and analyzed by the Dickinson FACS Calibur System (San Jose, CA) using emission filters of 515–545 nm for FITC (green) and 600 nm for PI (red). A total of 10 000 events were acquired for each sample (Kafil & Omidi, 2011).

Quantitative real-time PCR

The effect of GBA and GBA-SLNs on the expression of *Casp9* and *Bcl-xL* genes (as pro- and antiapoptotic markers, respectively) was studied by quantitative real-time PCR using the iQ5 real-time PCR detection system (Bio-Rad Laboratories Inc., Hercules, CA). Cells were treated with 100 µM GBA (intact or GBA-SLNs) and 3.13 µM doxorubicin (IC_{50} value in A549 cells) as a positive control (Ghasemi et al., 2013) for 48 h. Total RNAs from the negative control and treated cells were extracted using the RNeasy mini Kit (Qiagen, Hilden, Germany). The integrity of the extracted RNA and quality of *18s* rRNA and *23s* rRNA bounds was evaluated by agarose gel electrophoresis and the purity of RNA was examined by optical density measurement (A260/A280 ratio) with nano drop instrument (ND 1000, NanoDrop Technologies, Inc., Wilmington, DE). For complementary DNA (cDNA) synthesis, 1 µg of RNA samples was used based on our previous work (Vandghanooni et al., 2011). Primers were designed using Oligo 7.56 (Molecular Biology Insights, Inc, Colorado Springs, CO) from published Gene Bank sequences as following: C*asp9* gene (Gene Bank accession no: NM_001229.2): forward 5′-TGCTGCGTGGT GGTCATTCTC-3′ and reverse 5′-CCGACACAGGGCATCC ATCTG-3′ with an annealing temperature of 62 °C to amplify a 94 bp fragment; *Bcl-xL* gene (Gene Bank accession no: NM_138578.1): forward 5′-GTTCCCTTTCCTTCCATCC-3′ and reverse 5′-TAGCCAGTCCAGAGGTGAG-3′ with an annealing temperature of 60 °C to amplify a 123 bp fragment; *GAPDH* as the housekeeping gene (Gene Bank accession no: NM_002046.3): forward 5′-AAGCTCATTTCCTGGTATGA CAACG-3′ and reverse 5′-TCTTCCTCTTGTGCTCTTGCTG G-3′ with an annealing temperature of 62 °C to amplify a 126 bp fragment. All amplification reactions were performed in a total volume of 25 µl composed of 1 µl cDNA, 1 µl reverse and forward primers (100 nM), 12.5 µl 2X SYBER

green PCR Master Mix, and 10.5 µl RNAse/DNAse free water. Thermal cycling conditions were as follows: 1 cycle at 94 °C for 10 min, 40 cycles at 95 °C for 15 s, 60/62 °C for 30 s, and 72 °C for 25 s. Data were analyzed using the Pfaffl method and the CT values were normalized to the expression rate of *GAPDH* as a housekeeping gene (Vu et al., 2000).

Statistical analyses

All expressed data in this context represent the mean of at least three repeated experiments (error bars represent mean ± St Dev). An independent Student's *t*-test was used to compare mean differences between two independent groups and a one-way ANOVA was used for multiple comparisons. Where the differences between the means were significant, *post hoc* pair wise comparisons were carried out using Tukey multiple comparison tests (SPSS; version 13.0, SPSS Inc., Chicago, IL). The statistical significance was defined as $p<0.05$.

Results

Preparation and characterization of GBA-SLNs

In this investigation, SLNs were prepared using Precirol® ATO 5, stabilized using a surfactant, i.e. Tween 80 or Tween 20 and Poloxamer 407 as a co-surfactant. The size of the nanoparticles was generally smaller in the case of GBA-SLNs when compared with the blank SLNs. There is an obvious decrease of nanoparticle size with an increase of the oil phase surfactant. When 0.8% Tween 80 was used, we could not get particles with the size less than 150 nm; however, when 6% Tween 80 was used, we could get particles with the size less than 100 nm. Because of favorable results in terms of EE, particle size, and zeta potential, the next steps were focused on the formulations 10 and 19 for blank and drug-loaded SLNs, respectively. In the F19, the polydispersity index (PDI) was well below 0.14, indicating a narrow particle size distribution with the mean diameter of 92 nm that were also confirmed by SEM (Figure 2B); likewise F10 had a similar volume mean diameter and a PI of 0.115 ± 0.023. Under the physiologic pH condition (7.4), zeta potential of selected formulation, F19 and F10, was -23.39 ± 1.14 and -11.28 ± 2.06, respectively (Figure 2C and D).

EE and DL

Table 1 shows the influence of oil phase and aqueous phase surfactants on EE. There is an evident improvement of EE with an increase in the oil phase surfactant. However, the type of oil phase surfactant and the percentage of aqueous phase surfactant showed no significant effects on EE and DL ($p > 0.05$). The EE was 68.25 for SLNs prepared with 0.8% Tween 80. When 6% Tween 80 was used, EE was increased to 98.89 in SLNs prepared with precirol. SLNs prepared with

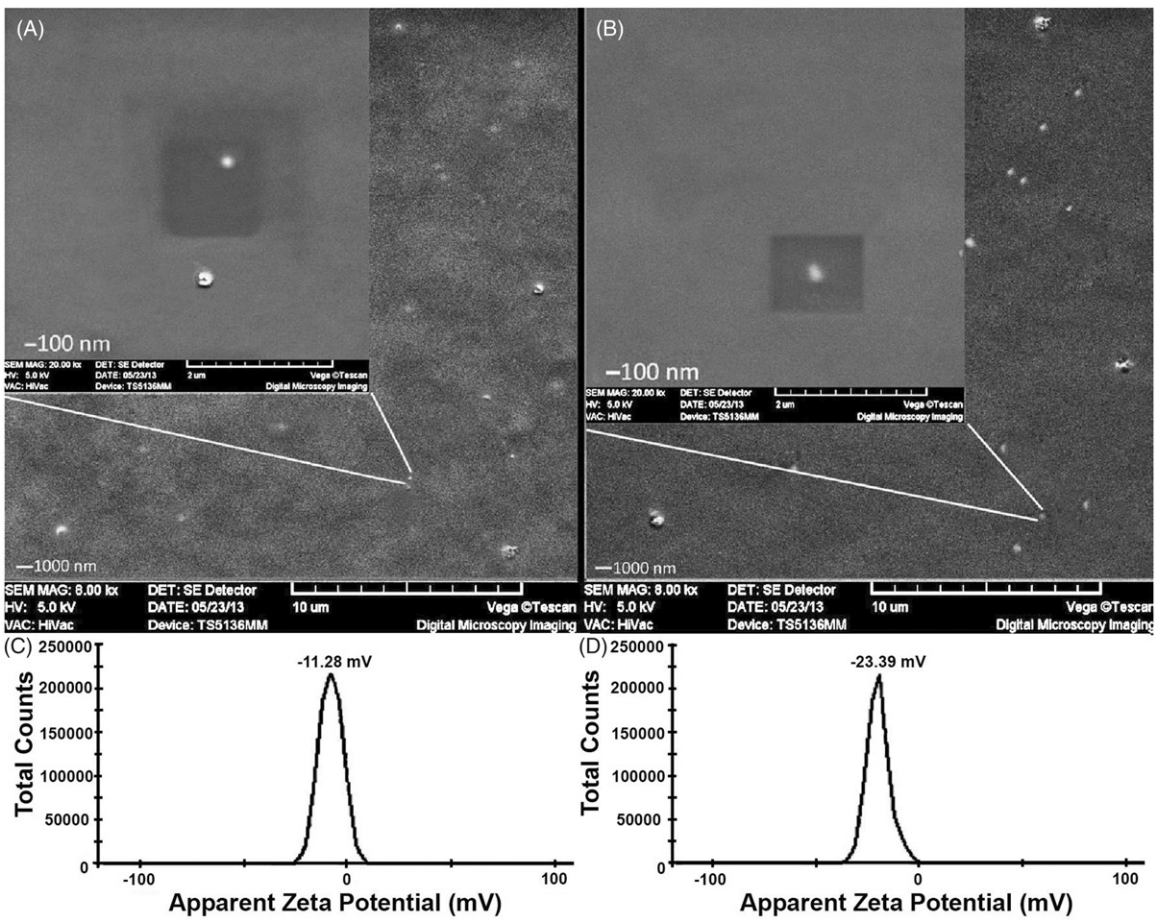

Figure 2. SEM images of (A) blank SLNs (F10) and (B) GBA-SLNs (F19), and zeta potential of (C) F10 and (D) F19. (F10) and (F19) represent the formulation code of 10 and 19 for blank SLNs and GBA-SLN, respectively.

Table 1. Composition, particle size, and encapsulation efficiency (EE) of galbanic acid-loaded SLNs formulation.

Formulation code	Lipid type and concentration (g)	Drug concentration (g)	Oil phase surfactant type and concentration (g)	Aqueous phase surfactant concentration[a] (g)	Particle size (nm)	Poly-dispersity	Encapsulation efficiency (EE %)	Drug loading (DL, mg/g)	Drug content (%)
Blank SLNs									
F1	Precirol (0.55)	–	Tween 20 (0.01)	0.52	183 ± 8.13	0.558 ± 0.131	–	–	–
F2	Precirol (0.55)	–	Tween 20 (0.05)	0.68	164 ± 6.24	0.482 ± 0.142	–	–	–
F3	Precirol (0.60)	–	Tween 20 (0.07)	0.75	132 ± 4.14	0.332 ± 0.121	–	–	–
F4	Precirol (0.58)	–	Tween 20 (0.10)	0.83	101 ± 3.03	0.227 ± 0.128	–	–	–
F5	Precirol (0.58)	–	Tween 20 (0.13)	0.88	98 ± 1.88	0.189 ± 0.109	–	–	–
F6	Precirol (0.62)	–	Tween 20 (0.15)	0.92	83 ± 2.04	0.115 ± 0.089	–	–	–
F7	Precirol (0.60)	–	Tween 80 (0.01)	0.43	203 ± 9.91	0.449 ± 0.79	–	–	–
F8	Precirol (0.61)	–	Tween 80 (0.06)	0.59	173 ± 7.68	0.332 ± 0.203	–	–	–
F9	Precirol (0.59)	–	Tween 80 (0.08)	0.68	140 ± 4.56	0.204 ± 0.194	–	–	–
F10	Precirol (0.59)	–	Tween 80 (0.10)	0.79	93 ± 2.78	0.115 ± 0.023	–	–	–
GBA-loaded SLNs									
F11	Precirol (0.59)	0.043	Tween 20 (0.01)	0.48	162 ± 7.01	0.444 ± 0.109	77.13 ± 3.34	34.21 ± 0.45	3.02
F12	Precirol (0.62)	0.039	Tween 20 (0.06)	0.55	155 ± 5.34	0.502 ± 0.151	82.22 ± 2.98	32.01 ± 0.23	2.52
F13	Precirol (0.65)	0.049	Tween 20 (0.09)	0.69	125 ± 3.89	0.253 ± 0.105	88.42 ± 1.88	42.74 ± 0.12	2.90
F14	Precirol (0.60)	0.047	Tween 20 (0.10)	0.78	94 ± 1.83	0.177 ± 0.221	91.55 ± 4.43	43.1 ± 0.36	2.75
F15	Precirol (0.63)	0.044	Tween 20 (0.13)	0.81	90 ± 1.33	0.142 ± 0.231	94.39 ± 3.99	42.68 ± 0.45	2.54
F16	Precirol (0.59)	0.045	Tween 20 (0.15)	0.88	78 ± 1.54	0.121 ± 0.091	96.69 ± 2.65	43.28 ± 0.25	2.58
F17	Precirol (0.61)	0.039	Tween 80 (0.01)	0.58	151 ± 7.34	0.331 ± 0.171	68.25 ± 5.31	26.61 ± 0.46	2.09
F18	Precirol (0.63)	0.040	Tween 80 (0.05)	0.62	122 ± 6.52	0.373 ± 0.274	86.11 ± 5.24	34.44 ± 0.33	2.53
F19	Precirol (0.58)	0.045	Tween 80 (0.08)	0.64	92 ± 3.302	0.135 ± 0.041	98.89 ± 3.67	44.5 ± 0.28	4.13
F20	Precirol (0.63)	0.039	Tween 80 (0.12)	0.88	77 ± 3.44	0.101 ± 0.108	96.09 ± 4.43	37.4 ± 0.37	1.37

Data are expressed as mean ± SD ($n = 3$).
[a]Poloxamer 407 was used as the aqueous phase surfactant in all formulations.

precirol containing 6.3% of Tween 80 exhibited the highest DL values (44.5 ± 0.28 mg/g). In the F19 formulations, EE was higher than 98%, which was selected for *in vitro* release and bioactivity analysis.

In vitro release, kinetic release, and drug leakage studies

The *in vitro* release behavior of GBA-SLNs is presented as the cumulative percentage release of GBA (Figure 3). The freshly prepared suspension in different pHs (7.4 and 5.6) and temperatures (37 ± 0.5 °C and 24 ± 2 °C) had a less than 6% drug released within the initial 24 h, followed by a relatively faster release phase lasting for 144 h. Then a more gradual slow release was observed in all conditions. However, drug release pattern in different pHs and temperatures was a little different. In the lower pH and higher temperature, the release became faster. At 37 ± 0.5 °C, in pHs 7.4 and 5.6 over 350 h, the cumulative drug released was 12.44 ± 0.43% and 13.22 ± 0.26%, respectively. While at 24 ± 0.2 °C in pHs 7.4 and 5.6 over 350 h, the cumulative drug released was lower than 8 and 9%, respectively. However, all the differences were not significant ($p > 0.05$). The plain GBA control exhibited a rapid release with 33% drug released within 12 h. The release was almost complete (98.8%) by 48 h. Table 2 represents various kinetics models used to fit the GBA release profile. As shown, GBA release profile was best fit with the Weibull model. Results from drug leakage studies showed that the leakage profile of GBA from SLNs was relatively greater at higher temperature. It was found that after 3 months of storage the leaked drug in the aqueous phase was lower than 6 and 9% at 4 and 24 °C, respectively (Table 3).

Physical stability studies

Formulation composed of 3.1% (w/v) GBA, a surfactant system consisting of 6.3% Tween 80 and 90% Poloxamer 407 in a solid lipid matrix of 82% precirol, was placed on long-term stability at 4 °C and 24 °C for up 3 months. After three month, samples were withdrawn and the nano-suspension was checked for any potential aggregation, and SLNs were evaluated in terms of size, PI, and EE. Stability studies showed that in the usual dispersed aqueous medium (distilled water), coacervation and precipitation of lipid did not occur.

The polydispersity index values of 0.147 ± 0.03 and 0.214 ± 0.05 were obtained for the samples kept at 4 °C and 24 °C after 3-month storage, respectively. There was no significant change in the volume mean particle size upon storing (Figure 4; $p > 0.05$). Moreover, after 3-month storage at 4 °C and 24 °C, DL was 42.04 ± 0.74 and 40.05 ± 0.42 mg/g, respectively, that compared with the fresh one (44.5 ± 0.28 mg/g) showed no significant differences ($p > 0.05$). Totally, storage at a low temperature provided better stability with regard to both particle size and DL. The small decrease in DL is indicative of an insignificant drug expulsion from the SLNs. This is a typical feature of SLN formulations and has been illustrated previously.

MTT assays

The cytotoxicity of GBA (intact and SLNs) was investigated by MTT assay and is presented in Figure 5. The results showed that GBA was able to inhibit A549 cells growth rate as well as 5% DMSO (positive control) with an IC_{50} value of approximately 75, 62, and 50 μM at 24 h, 48 h, and 72 h, respectively. Although GBA-SLNs could also inhibit the

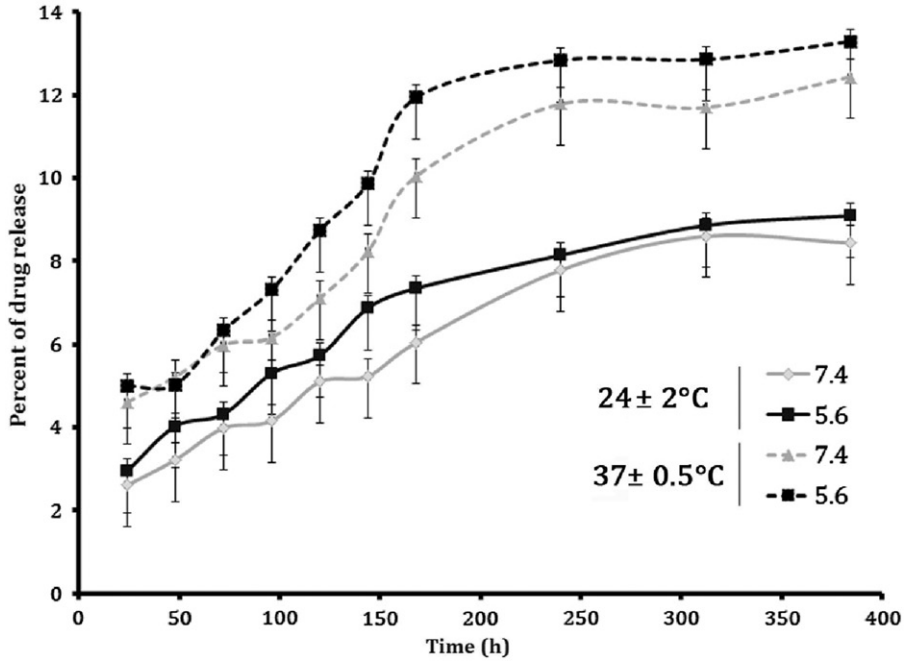

Figure 3. Cumulative release of GBA from SLNs under medium containing 0.3% Tween 80, at different temperatures (24 and 37 °C) and pHs (7.4 and 5.6) after 16 h (384 h). All data represent the mean of at least three-recorded OD (error bars represent mean ± SD).

Table 2. The kinetics models used to fit the release data.

		Coefficient of determination (R^2)			
		24 ± 2 °C		37 ± 0.5 °C	
Kinetic model	Equation	pH 5.6	pH 7.4	pH 5.6	pH 7.4
Zero order	$F = k_0 t$	0.763	0.721	0.795	0.773
First order	$Ln(1-F) = -k_f t$	0.831	0.792	0.873	0.829
Higuchi	$F = k_H\sqrt{t}$	0.918	0.901	0.928	0.906
Weibull	$Ln[-Ln(1-F)] = -\beta Lnt_d + \beta Lnt$	0.978	0.974	0.983	0.977
Hixson–Crowell	$1-\sqrt[3]{1-F} = k_{1/3}t$	0.858	0.838	0.862	0.854

Parameters of models were obtained by linear regression. F represents fraction of drug released up to time t. The k_0, kf, k_H, and $k_{1/3}$ are parameters of the models. Ln, natural logarithm.

Table 3. Physical stability and drug leakage studies of the GBA-SLNs.

	Size volume average (nm)	Polydispersity index (PI)	Encapsulation efficiency (%)	Drug leakage (%)
Fresh GBA-SLNs	92 ± 4	0.135 ± 0.04	98.89 ± 0.19	–
GBA-SLNs in 4 °C after 3 month	93.1 ± 5	0.147 ± 0.03	93.21 ± 0.26	5.68
GBA-SLNs in 24 °C after 3 month	99.3 ± 6	0.214 ± 0.05	90.7 ± 0.29	8.19

Error bars represent mean ± standard deviation (n=3).

growth rate of A549 cells, the effect is perceived after 48 h of treatment (Figure 5B and C) showing somewhat delayed response. Interestingly, neither plain GBA nor GBA-SLNs showed no toxicity on HUVEC as a non-proliferative healthy cell lines in the concentration used for the experiments. This may approve its application as a selective and suitable drug delivery nanoparticle against cancerous cells. According to the obtained results, some prepared blank SLNs using Tween 20 were excluded due to the cytotoxicity properties but the other blank SLNs that prepared using Tween 80 showed no toxicity effects against both cell lines (data not shown).

DAPI staining

Induction of apoptosis upon treatment of A549 cells and HUVEC with GBA and GBA-SLNs was also investigated by microscopic analysis of DAPI-stained cells. As it is clearly shown in Figure 6, apoptotic cells are apparent in both positive control and GBA-treated cells. The extent of fragmentation in the chromatin and DNA rings within the nucleus (Eskandani et al., 2014) of GBA-SLN-treated cells was higher than GBA-treated cells after 48 h of treatment. This may be due to slow release of GBA from nanoparticles as we had similar results with MTT assay where GBA-SLNs affected cell viability after 48 h as compared with 24 h with

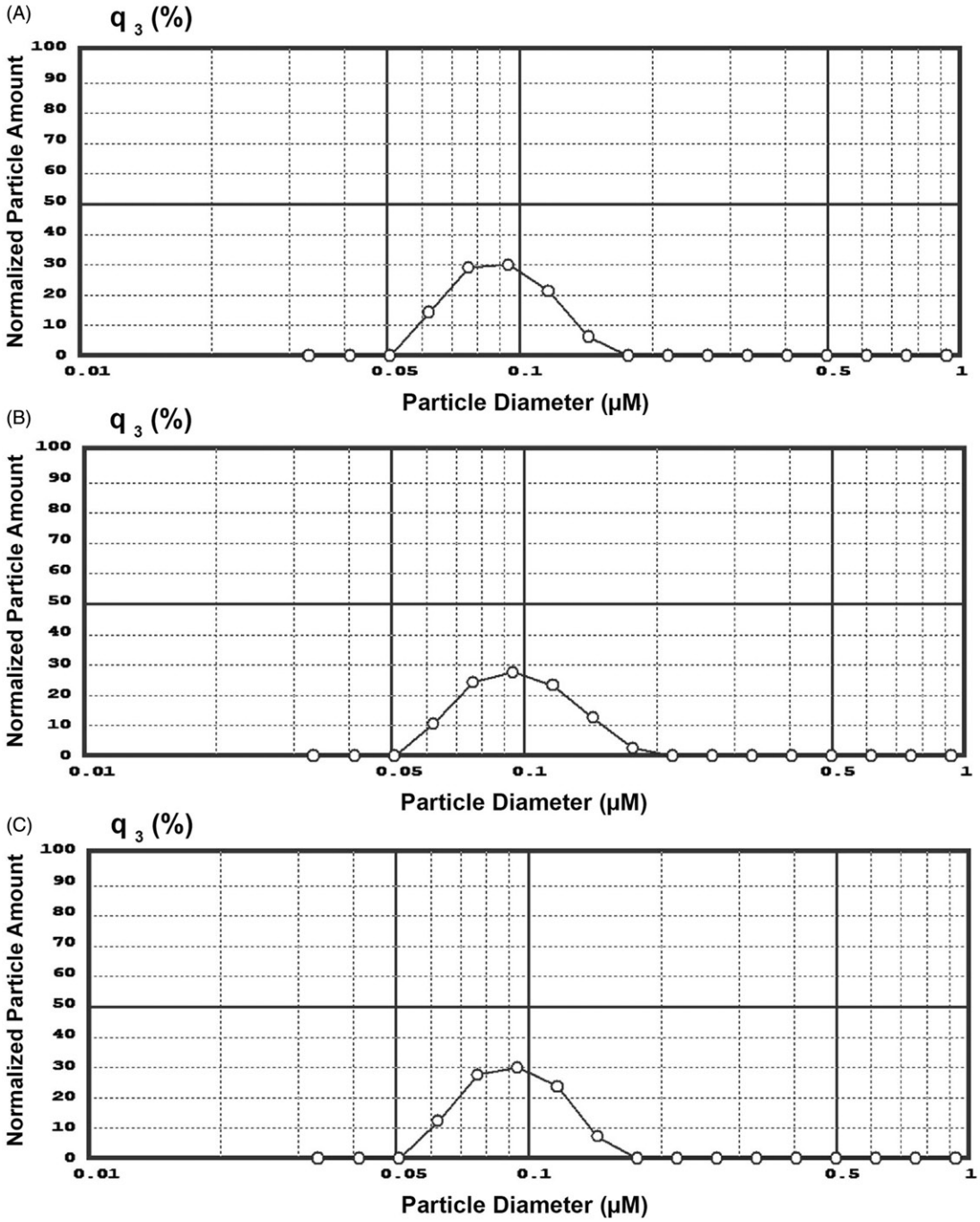

Figure 4. The differences in formulated SLNs size between the initial (A) and 3 months after storage at (B) 4 °C and (C) 24 °C were not found to be statistically significant.

free GBA. Interestingly, the fragmented chromatin in the nucleus of HUVEC treated with GBA and GBA-SLNs was rarely seen, also confirming the MTT results. In addition, light microscopic observations illustrated that the treated and untreated cells have distinct morphologic differences in the number and appearance of normal and dead cells.

Alkaline comet assay

To detect primary DNA damage induced by GBA and GBA-SLNs, alkaline comet assay was employed. As shown in Figure 7, GBA and GBA-SLN-treated A549 cells demonstrated significant single-strand breakage of DNA while no double- or single-strand DNA breakage was observed within healthy control cells. However, those treated with GBA or hydrogen peroxide showed DNA to some extent in the comet tails. Single-strand DNA cleavage in GBA-treated cells was slightly higher than GBA-loaded-treated cells (Figure 7E). Statistical analysis of percentage of tail DNA/Head DNA confirmed significant differences ($p < 0.05$) among untreated, plain GBA, and GBA-SLN-treated A549 cells (Figure 7E). However, insignificant differences ($p > 0.05$) between hydrogen peroxide and GBA-treated A549 cells were seen. Statistical analysis confirmed

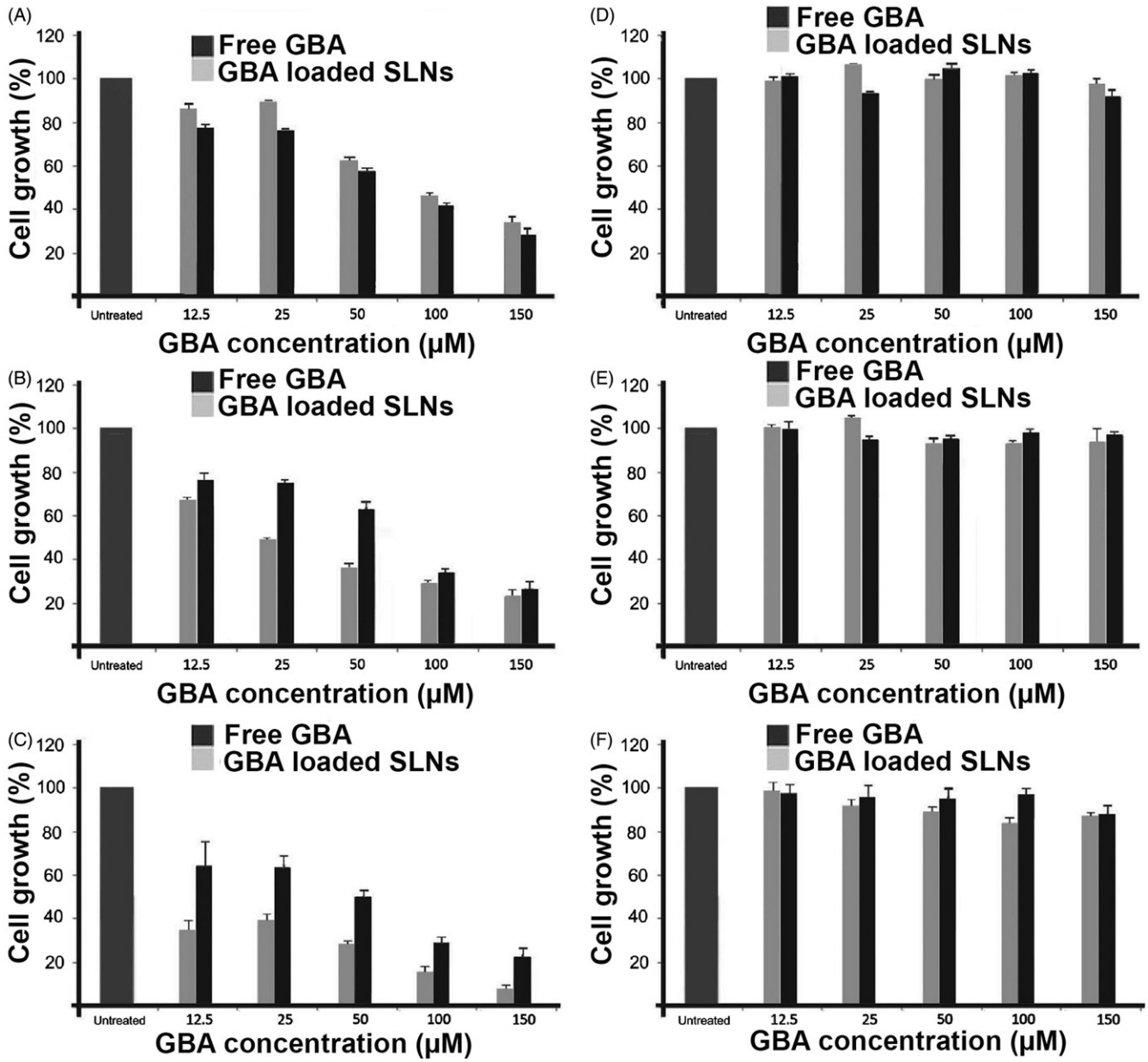

Figure 5. Inhibition properties of plain GBA (black) and GBA-SLNs (gray) on A549 human lung epithelial carcinoma after (A) 24 h, (B) 48 h, and (C) 72 h. (D), (E), and (F) MTT result of treatment of plain GBA (black) and GBA-SLNs (gray) on HUVEC after 24 h and 48 h and 72 h, respectively. Error bars represent SD (n=3).

insignificant differences ($p > 0.05$) between untreated and GBA or GBA-SLN-treated HUVEC.

DNA fragmentation assay

Gel electrophoresis (Figure 8) showed the formation of the 200 bp DNA ladder in GBA and GBA-SLN-treated A549 cells, which is evident when apoptosis occur. Therefore, the cyto/genotoxic effect of the GBA or GBA-SLNs was mediated mostly via the induction of apoptosis (Hamishehkar et al., 2014). Although hydrogen peroxide causes DNA fragmentation in both cell types, surprisingly, GBA or GBA-SLNs only led in DNA fragmentation in A549 cells and not in HUVEC. However, the qualitative results showed no significant differences between the fragmentation level in GBA and GBA-SLN-treated cells.

Flow cytometry analysis of apoptosis

We also followed translocation of phosphatidylserine (PS) from the inner layer of the cell membrane to the external layer using FITC-labeled annexin V in treated cells by flow cytometry (Vandghanooni et al., 2013). Incidence of early/late stages of apoptosis within A549 cells treated with both plain GBA and GBA-SLNs was observed. In comparison with untreated cells, treated cells with both treatments showed significant increases ($p < 0.05$) in the proportion of cells entering early and/or late apoptotic stages. Although after 48 h incubation, incidence of late apoptosis in GBA-treated cells was higher than GBA-SLN-treated cells (37.48% versus 20.05%) but GBA-SLN impacts in the induction of early stage of apoptosis were significantly greater than plain GBA (19.03% versus 10.04%). This result approved the sustained

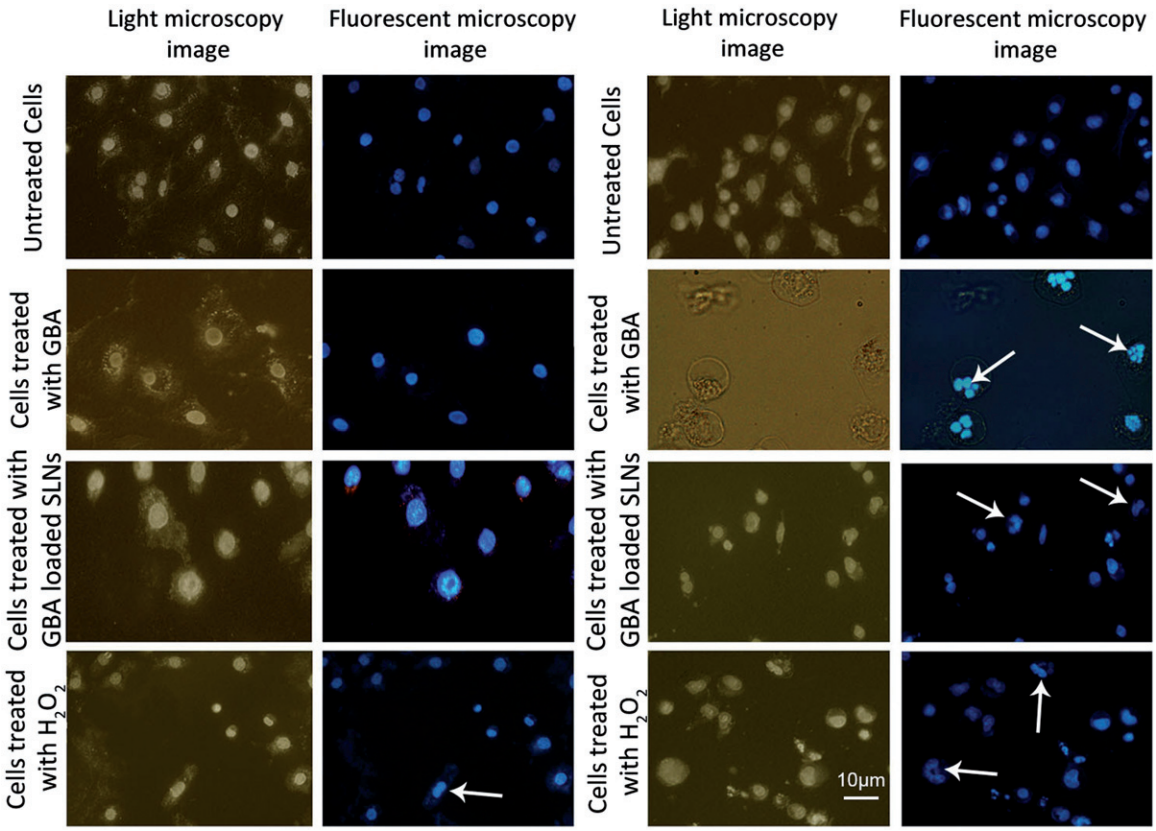

Figure 6. Light and fluorescent microscopy images of A549 cells and HUVEC stained with DAPI; (A) the HUVEC and (B) A549 cell line are shown. The arrows show fragmented nucleus in the treated cells.

and prolonged impact of GBA-SLNs compared with the plain GBA (Figure 9).

Bcl-*xL* and *Casp 9* genes transcript relative quantification

Different quantitative expressions of *Casp 9* gene, a pro-apoptosis gene, and *Bcl-xL* gene, a pro-survival gene, in GBA and GBA-SLNs confirmed the molecular mechanism of apoptosis (Tsujimoto et al., 2005). Figure 10 shows the relative quantification of *Bcl-xL* and *Casp 9* genes. Statistical analysis of the data demonstrated that quantitative expression of *Casp 9* gene in GBA and GBA-SLN-treated cells is significantly higher than untreated cells ($p < 0.05$). In addition, the results demonstrated that *Bcl-xL* gene is down-regulated in GBA and GBA-SLN-treated cells compared with untreated cells ($p < 0.05$). Down-regulation of pro-survival gene together with the up-regulation of pro-apoptosis gene demonstrated that apoptosis might occur in the plain GBA and GBA-SLN-treated cells.

Discussion

Coumarins as the anticipative medicinal compounds are of common occurrence in the different parts of *ferula* genus including aerial parts, roots, and fruits (Iranshahi et al., 2010; Meng et al., 2013). GBA is a lipophilic sesquiterpene coumarin and possesses different approved pharmaceutical activities. Synergism effect of GBA with penicillin G and cephalexin (Shahverdi et al., 2007), erythrocyte aggregation inhibitory properties (Mansurov & Martirosov, 1988), hepatoprotective effects through liver redox potential improving (Syrov et al., 1990), inhibition of the nitric oxide (NO) production (Kohno et al., 2011), down-regulation of androgen receptors abundance in the prostate gland (Zhang et al., 2012), anti-leishmanial activity (Iranshahi et al., 2007), and farnesyl-transferase inhibition (Cha et al., 2011) have reported for the compound.

In our investigations, low solubility of the GBA in the medium was the most important issues during *in vitro* anticancer characterization. Hence, to increase its solubility in the aqueous medium and to improve its pharmaceutical behavior, we successfully formulated GBA-SLNs and evaluated its pharmaceutical and biological activities. It has been reported that the formulation procedure and the composition of SLNs have noteworthy influence on physicochemical features. During SLNs preparation, the speed of stirrer was found to affect the mean particle size. Increasing the stirring speed in the final step of homogenization from 12 000 rpm to 19 000 rpm for a 15 min decreased the mean particle size of SLNs significantly (data not shown). Application of Tween 20 and Tween 80 as the oil phase surfactant led to smaller size and steady state of GBA-SLNs (Ezzati Nazhad Dolatabadi et al., 2014), but we desired to use Tween 80 instead of Tween 20 after finding some evidences about geno/cytotoxicity effect of Tween 20 on A549 cell and HUVEC lines (Eskandani et al., 2013). Evaluation of nanoparticles showed that the particle size and drug loading of the SLNs

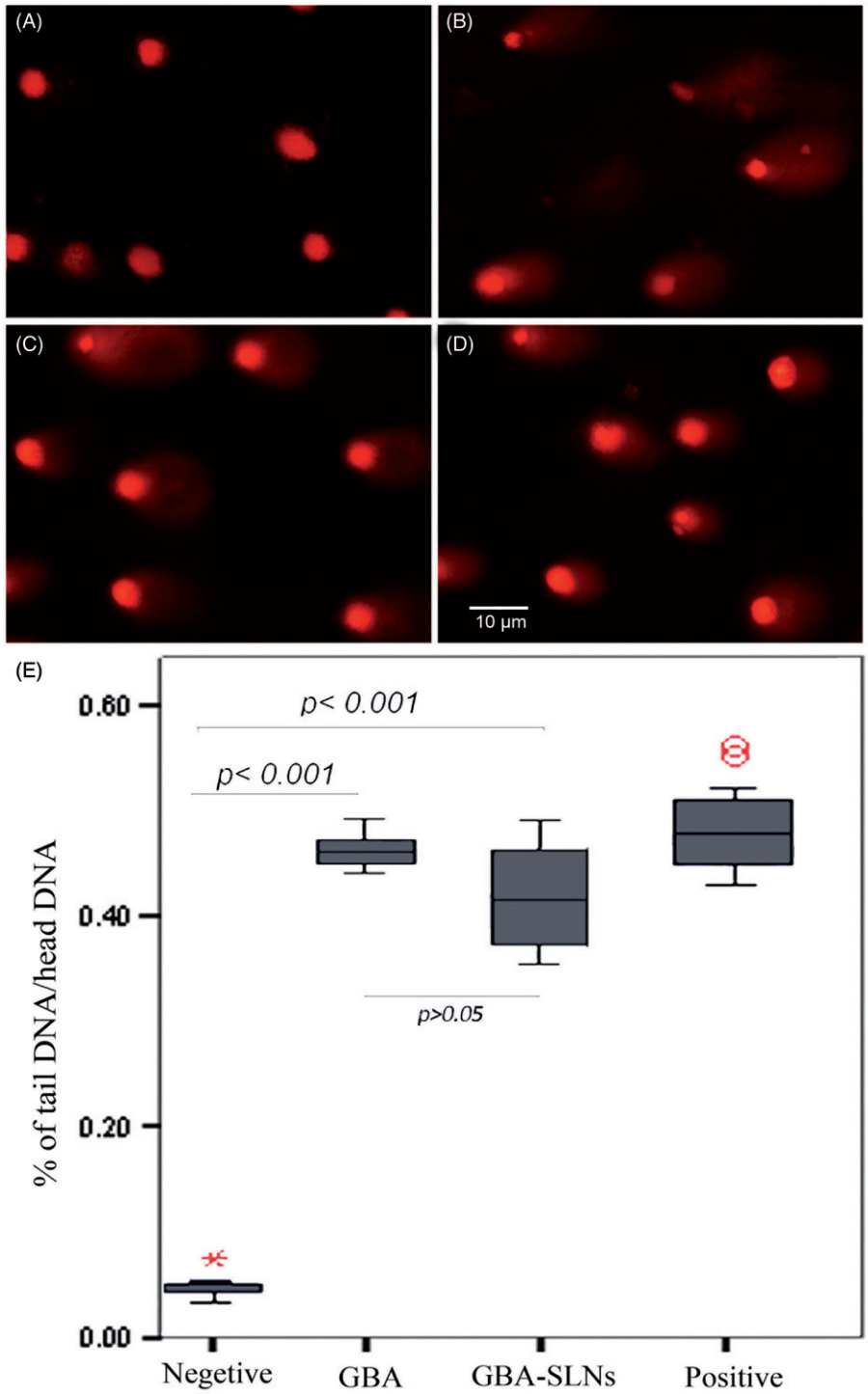

Figure 7. Photographic illustrations of comet assay after 48 h incubation. (A) Untreated A549 cells, (B) treated A549 cells by 200 µM H_2O_2 (positive control), (C) treated A549 cells by GBA, and (D) treated A549 cells by GBA-SLNs. (E) Box-plot graph of DNA tail/DNA head% is shown; the DNA cleavage level in GBA and GBA-SLN-treated cells is not as high as treated cells with 200 mM H_2O_2 but is significantly ($p<0.001$) higher than untreated cells.

are influenced by the oil phase surfactant concentrations (Müller et al., 2000). The data clearly showed that higher concentration of oil phase surfactant caused higher DL/EE and decreased the mean size of the SLNs. This notion previously has been shown (Abdelbary & Fahmy, 2009). This fact may attribute to the reduction of surface tension with higher lipophilic surfactant content that may lead to smaller particles (Hu et al., 2005). However, it should be considered that formulation of SLNs with higher concentration of surfactant ($\geq$ 10% w/v) shows some degrees of cytotoxicity on A549 cells (data not shown); hence, we considered 8% as a threshold and limited the surfactant level to eliminate the cytotoxic impact of blank SLNs.

We found very slow *in vitro* drug release in both room and body temperature that may be attributed to the hydrophobic nature of the SLNs and their surrounding polar environment, which do not permit water and drug diffusion in and out of the SLNs, respectively (Müller et al., 2000). The pattern of drug liberation revealed that 40% of drug was released within the first 24 h. This release may be referred to those drugs located on or near the particle surface, while the slow and uniform release could be caused by slow diffusion of the drugs from

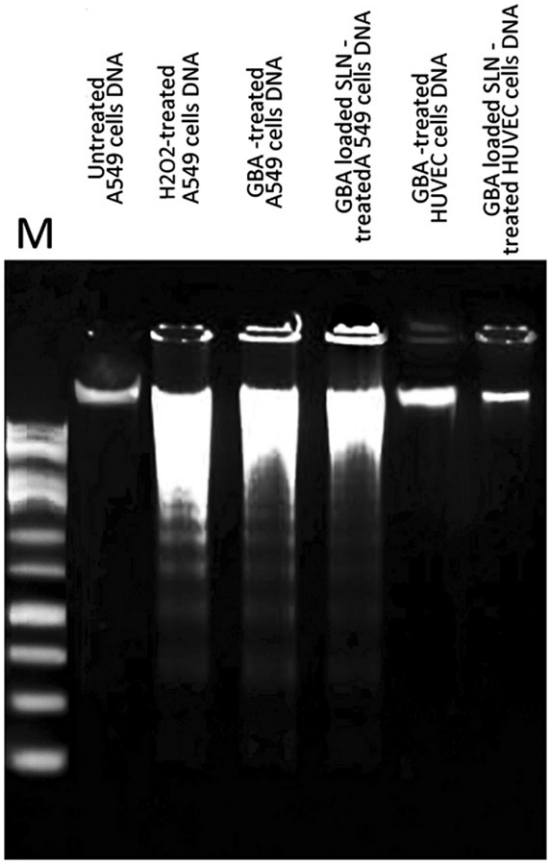

Figure 8. DNA ladder formation through gel electrophoresis in different treatments, and A549 cells and HUVEC. M, molecular marker.

the nanoparticles (Mehnert & Mäder, 2001). According to the previous study (Prombutara et al., 2012), we also observed non-significant higher *in vitro* drug release in pH 5.6 compared with pH 7.4. This observation makes SLNs as suitable particles for GBA delivery to the tumor microenvironment where the pH is lower than normal tissues.

MTT survival assay results showed that both GBA and GBA-SLNs decrease cell growth rate. Although intact GBA showed most effective anti-proliferative activity in early hours of treatment, but GBA-SLNs with lower content could induce ongoing apoptosis after 48 h. This result suggests that nanoparticles could be absorbed by the A549 cell membrane after earlier hours of the treatments. We also found that GBA had no effect on the structure and proliferation of non-proliferative HUVEC normal cell line. The results are in accordance with the previous study (Kim et al., 2011). According to the cytotoxicity and genotoxicity evaluation, the results displayed that blank SLNs showed no significant toxicity *in vitro* ($p > 0.05$). DAPI staining and DNA fragmentation assays showed that the DNA breakage or fragmentation in GBA and GBA-SLNs has occurred. However, we found the same degree of fragmentation in GBA and GBA-SLN-treated cells. In addition, significant double-strand breakage of DNA was observed in A549 cells by comet assay. Box-plot analysis of comet assay showed no significant differences between GBA and GBA-SLN-treated cells ($p > 0.05$). However, both drugs could induce significant fragmentation compared with the un-treated cells ($p < 0.05$). We also established that GBA could induce late apoptosis and even necrosis better than

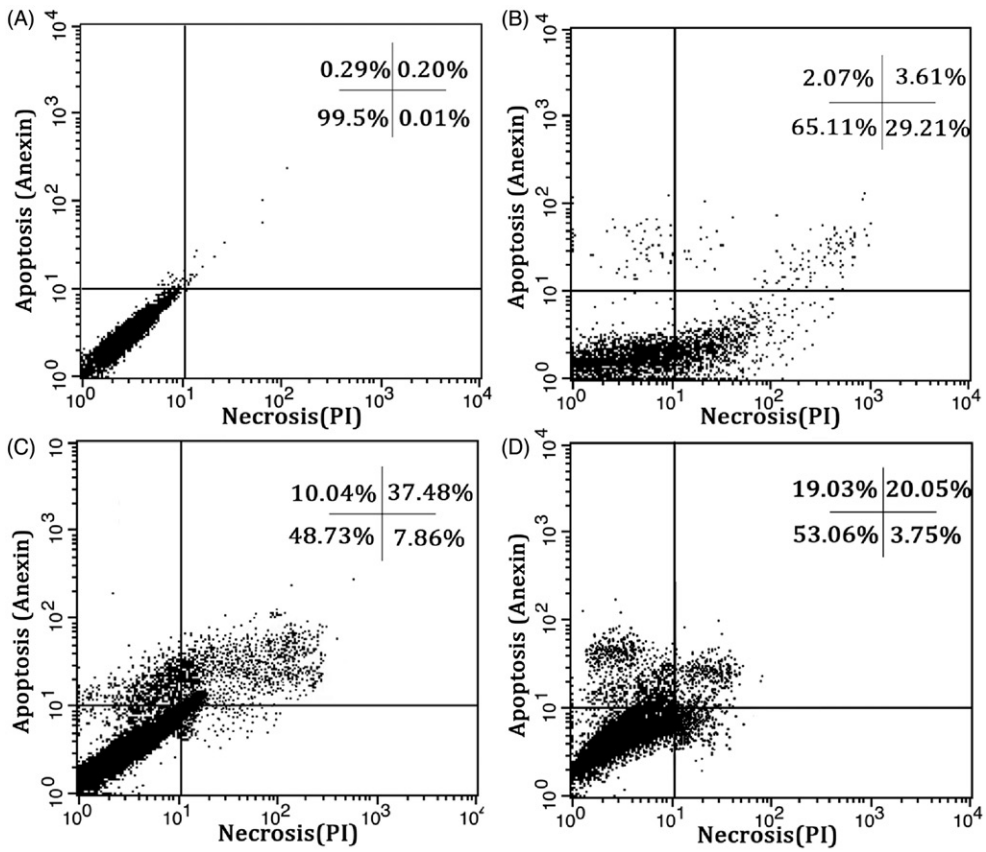

Figure 9. FITC-labeled annexin V flow cytometric detection of apoptosis in A549 cells. (A) Untreated control cells, (B) treated cells with 200 μM H_2O_2 as a positive control, (C) treated cells with GBA, and (D) treated cells with GBA-loaded SLNs.

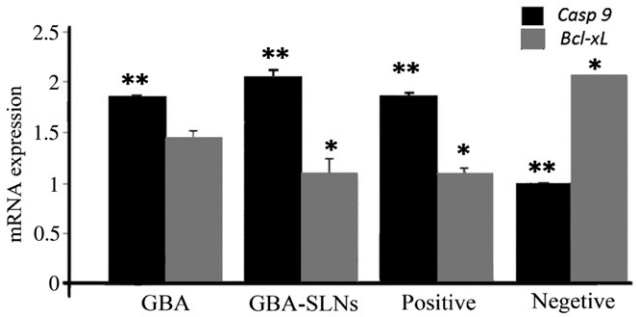

Figure 10. Differential expression levels of *Casp 9* and *Bcl-xL* genes in plain GBA, GBA-SLNs, and doxorubicin (as positive control). * and ** represent significant differences ($p < 0.05$).

GBA-SLNs after 48 h, yet incidence of early stages of apoptosis in GBA-SLN-treated A549 cells was significantly greater than plain GBA-treated cells ($p < 0.05$). This finding could be a good reason for the controlled release properties of SLNs.

Finally, different quantitative expression levels of *Casp 9* pro-apoptosis gene and *Bcl-xL* pro-survival gene in GBA and GBA-SLNs clear the molecular mechanism of apoptosis. The results demonstrate that GBA-SLNs could better down-regulate *Bcl-xL* gene and up-regulate *Casp 9* gene compared with plain GBA. However, quantitative gene expression differences were not significant.

Conclusions

For the first time, GBA-SLNs were successfully formulated by the simple hot homogenization method with high EE (>98%), nano-ranged size, and highly monodispersed distribution. Biocompatibility of blank SLNs against A549 cells and HUVEC was confirmed by geno/cytotoxicity assays. Neither plain GBA nor GBA-SLNs showed cytotoxic effect on HUVEC while exerted significant impact on A549 cells, whereby after 48 h, GBA-SLNs had a higher impact. Conclusively, GBA can be uptaken by the cells as well as slowly released from nanoparticles after accumulation in acidified microenvironment of tumor cell, as shown by our data. Based on the obtained result, in the current study and comparison of the effects of plain GBA and GBA-SLNs, we concluded that formulation of the water insoluble GBA into the SLNs makes it very effective due to the increasing drug solubility and release time.

Declaration of interest

The authors declare that there are no conflicts of interest. Authors would like to thank Research Center for Pharmaceutical Nanotechnology (RCPN), Tabriz University of Medical Sciences, Tabriz, Iran, for supporting this project (Grant no. 90011, which is a part of PhD thesis no. 90/011/101/1).

References

Abdelbary G, Fahmy RH. (2009). Diazepam-loaded solid lipid nanoparticles: Design and characterization. *AAPS PharmSciTech* 10: 211–19.

Bedniak AE. (1962). On the problem of the isolation of galbanic acid from *Ferula gumosa* Boiss. roots. *Aptechn Delo* 12:28–34.

Cha MR, Choi YH, Choi CW, et al. (2011). Galbanic acid, a cytotoxic sesquiterpene from the gum resin of *Ferula asafoetida*, blocks protein farnesyltransferase. *Planta Med* 77:52–4.

Das S, Ng WK, Tan RB. (2012). Are nanostructured lipid carriers (NLCs) better than solid lipid nanoparticles (SLNs): Development, characterizations and comparative evaluations of clotrimazole-loaded SLNs and NLCs? *Eur J Pharm Sci* 47:139–51.

Eskandani M, Golchai J, Pirooznia N, et al. (2010). Oxidative stress level and tyrosinase activity in vitiligo patients. *Indian J Dermatol* 55: 15–19.

Eskandani M, Hamishehkar H, Ezzati Nazhad Dolatabadi J. (2013). Cyto/genotoxicity study of polyoxyethylene (20) sorbitan monolaurate (Tween 20). *DNA Cell Biol* 32:498–503.

Eskandani M, Hamishehkar H, Ezzati Nazhad Dolatabadi J. (2014). Cytotoxicity and DNA damage properties of tert-butylhydroquinone (TBHQ) food additive. *Food Chem* 153:315–20.

Eskandani M, Nazemiyeh H. (2014). Self-reporter shikonin-Act-loaded solid lipid nanoparticle: Formulation, physicochemical characterization and geno/cytotoxicity evaluation. *Eur J Pharm Sci* 59:49–57.

Ezzati Nazhad Dolatabadi J, Hamishehkar H, Eskandani M, et al. (2014). Formulation, characterization and cytotoxicity studies of alendronate sodium-loaded solid lipid nanoparticles. *Colloids Surf B* 117:21–8.

Ghaffari S, Varshosaz J, Saadat A, et al. (2011). Stability and antimicrobial effect of amikacin-loaded solid lipid nanoparticles. *Int J Nanomed* 6:35–43.

Ghasemi S, Davaran S, Sharifi S, et al. (2013). Comparison of cytotoxic activity of L778123 as a farnesyltranferase inhibitor and doxorubicin against A549 and HT-29 cell lines. *Adv Pharm Bull* 3:73–7.

Hamishehkar H, Khani S, Kashanian S, et al. (2014). Geno- and cytotoxicity of propyl gallate food additive. *Drug Chem Toxicol* 37: 241–6.

Han J, Chen T-X, Branford-White CJ, et al. (2009). Electrospun shikonin-loaded PCL/PTMC composite fiber mats with potential biomedical applications. *Int J Pharm* 382:215–21.

Hanafi-Bojd MY, Iranshahi M, Mosaffa F, et al. (2011). Farnesiferol A from *Ferula persica* and galbanic acid from *Ferula szowitsiana* inhibit P-glycoprotein-mediated rhodamine efflux in breast cancer cell lines. *Planta Med* 77:1590–3.

Hu F-Q, Jiang S-P, Du Y-Z, et al. (2005). Preparation and characterization of stearic acid nanostructured lipid carriers by solvent diffusion method in an aqueous system. *Colloids Surf B* 45: 167–73.

Huang G, Zhang N, Bi X, et al. (2008). Solid lipid nanoparticles of temozolomide: Potential reduction of cardial and nephric toxicity. *Int J Pharm* 355:314–20.

Iranshahi M, Arfa P, Ramezani M, et al. (2007). Sesquiterpene coumarins from *Ferula szowitsiana* and *in vitro* antileishmanial activity of 7-prenyloxycoumarins against promastigotes. *Phytochemistry* 68:554–61.

Iranshahi M, Masullo M, Asili A, et al. (2010). Sesquiterpene coumarins from *Ferula gumosa*. *J Nat Prod* 73:1958–62.

Kafil V, Omidi Y. (2011). Cytotoxic impacts of linear and branched polyethylenimine nanostructures in A431 cells. *Bioimpacts* 1:23–30.

Kheradmandnia S, Vasheghani-Farahani E, Nosrati M, et al. (2010). Preparation and characterization of ketoprofen-loaded solid lipid nanoparticles made from beeswax and carnauba wax. *Nanomedicine: NBM* 6:753–9.

Kim KH, Lee HJ, Jeong SJ, et al. (2011). Galbanic acid isolated from *Ferula assafoetida* exerts *in vivo* antitumor activity in association with antiangiogenesis and antiproliferation. *Pharm Res* 28:597–609.

Kohno S, Murata T, Sugiura A, et al. (2011). Methyl galbanate, a novel inhibitor of nitric oxide production in mouse macrophage RAW264.7 cells. *J Nat Med* 65:353–9.

Li Y, Dong L, Jia A, et al. (2006). Preparation and characterization of solid lipid nanoparticles loaded traditional Chinese medicine. *Int J Biol Macromol* 38:296–9.

Luo Y, Chen D, Ren L, et al. (2006). Solid lipid nanoparticles for enhancing vinpocetine's oral bioavailability. *J Control Release* 114: 53–9.

Mansurov MM, Martirosov MS. (1988). Effect of the sodium salt of galbanic acid on thrombocyte aggregation. *Farmakol Toksikol* 51: 47–8.

Matthaiou EI, Barar J, Sandaltzopoulos R, et al. (2014). Shikonin-loaded antibody-armed nanoparticles for targeted therapy of ovarian cancer. *Int J Nanomed* 9:1855–70.

Mehnert W, Mäder K. (2001). Solid lipid nanoparticles: Production, characterization and applications. *Adv Drug Deliv Rev* 47:165–96.

Meng H, Li G, Huang J, et al. (2013). Sesquiterpene coumarin and sesquiterpene chromone derivatives from *Ferula ferulaeoides* (Steud.) Korov. *Fitoterapia* 86:70–7.

Müller RH, Mäder K, Gohla S. (2000). Solid lipid nanoparticles (SLN) for controlled drug delivery – A review of the state of the art. *Eur J Pharm Biopharm* 50:161–77.

Nath M, Vats M, Roy P. (2013). Tri- and diorganotin(IV) complexes of biologically important orotic acid: Synthesis, spectroscopic studies, *in vitro* anticancer, DNA fragmentation, enzyme assays and *in vivo* antiinflammatory activities. *Eur J Med Chem* 59:310–21.

Parveen R, Ahmad FJ, Iqbal Z, et al. (2013). Solid lipid nanoparticles of anticancer drug andrographolide: Formulation, *in vitro* and *in vivo* studies. *Drug Dev Ind Pharm* 40:1206–12.

Prombutara P, Kulwatthanasal Y, Supaka N, et al. (2012). Production of nisin-loaded solid lipid nanoparticles for sustained antimicrobial activity. *Food Control* 24:184–90.

Rostami E, Kashanian S, Azandaryani AH, et al. (2014). Drug targeting using solid lipid nanoparticles. *Chem Phys Lipids* 181:56–61.

Schwarz C, Mehnert W. (1999). Solid lipid nanoparticles (SLN) for controlled drug delivery. II. Drug incorporation and physicochemical characterization. *J Microencapsul* 16:205–13.

Shahverdi AR, Fakhimi A, Zarrini G, et al. (2007). Galbanic acid from *Ferula szowitsiana* enhanced the antibacterial activity of penicillin G and cephalexin against *Staphylococcus aureus*. *Biol Pharm Bull* 30: 1805–7.

Shi F, Zhao JH, Liu Y, et al. (2012). Preparation and characterization of solid lipid nanoparticles loaded with frankincense and myrrh oil. *Int J Nanomed* 7:2033–43.

Singh NP, Mccoy MT, Tice RR, et al. (1988). A simple technique for quantitation of low levels of DNA damage in individual cells. *Exp Cell Res* 175:184–91.

Suresh G, Manjunath K, Venkateswarlu V, et al. (2007). Preparation, characterization, and *in vitro* and *in vivo* evaluation of lovastatin solid lipid nanoparticles. *AAPS PharmSciTech* 8:E162–70.

Syrov VN, Khushbaktova ZA, Nabiev AN. (1990). The effect of galbanic acid on the course of experimental hepatitis. *Farmakol Toksikol* 53: 41–3.

Tiyaboonchai W, Tungpradit W, Plianbangchang P. (2007). Formulation and characterization of curcuminoids loaded solid lipid nanoparticles. *Int J Pharm* 337:299–306.

Tsujimoto K, Ono T, Sato M, et al. (2005). Regulation of the expression of caspase-9 by the transcription factor activator protein-4 in glucocorticoid-induced apoptosis. *J Biol Chem* 280:27638–44.

Van Engeland M, Nieland LJ, Ramaekers FC, et al. (1998). Annexin V-affinity assay: A review on an apoptosis detection system based on phosphatidylserine exposure. *Cytometry* 31:1–9.

Vandghanooni S, Eskandani M. (2011). Comet assay: A method to evaluate genotoxicity of nano-drug delivery system. *Bioimpacts* 1: 87–97.

Vandghanooni S, Eskandani M, Montazeri V, et al. (2011). Survivin-deltaEx3: A novel biomarker for diagnosis of papillary thyroid carcinoma. *J Cancer Res Ther* 7:325–30.

Vandghanooni S, Forouharmehr A, Eskandani M, et al. (2013). Cytotoxicity and DNA fragmentation properties of butylated hydroxyanisole. *DNA Cell Biol* 32:98–103.

Vu HL, Troubetzkoy S, Nguyen HH, et al. (2000). A method for quantification of absolute amounts of nucleic acids by (RT)-PCR and a new mathematical model for data analysis. *Nucleic Acids Res* 28: E18 (1–9).

Wang W, Zhu R, Xie Q, et al. (2012). Enhanced bioavailability and efficiency of curcumin for the treatment of asthma by its formulation in solid lipid nanoparticles. *Int J Nanomed* 7:3667–77.

Zhang Y, Kim KH, Zhang W, et al. (2012). Galbanic acid decreases androgen receptor abundance and signaling and induces G1 arrest in prostate cancer cells. *Int J Cancer* 130:200–12.

Zur Mühlen A, Schwarz C, Mehnert W. (1998). Solid lipid nanoparticles (SLN) for controlled drug delivery – Drug release and release mechanism. *Eur J Pharm Biopharm* 45:149–55.